IOP Publishing Journal of Physics: Conference Series **61** (2007) 931–935
doi:10.1088/1742-6596/61/1/185 International Conference on Nanoscience and Technology (ICN&T 2006)

Aid of Raman spectroscopy in diagnostics of MWCNT synthesised by Fe-catalysed CVD

M.G.Donato, G.Messina, S.Santangelo

INFM, Dipartimento di Meccanica e Materiali, Facoltà di Ingegneria, Università "Mediterranea", Località Feo di Vito, 89060 Reggio Calabria, Italy

S.Galvagno, C.Milone, A.Pistone

Dipartimento di Chimica Industriale e Ingegneria dei Materiali, Facoltà di Ingegneria, Università di Messina, Contrada di Dio, 98166 Messina, Italy

saveria.santangelo@unirc.it

Abstract. This work shows that a set of quality indicators (QI), able to reliably monitor the basic characteristics of carbon nanotubes (CNT) grown by of Fe-catalysed chemical vapour deposition (CVD), can be derived from Raman spectroscopy (RS) measurements. Multi-walled nanotubes, prepared at 750 °C in C_2H_6+H_2 mixture over 20%Fe/SiO_2 catalyst, are demonstratively considered. By quantitatively analysing the spectra measured in the 100–3100 cm^{-1} range, information is obtained on level of defectiveness and degree of smoothness of C deposits, as well as, on relative amount of Fe-nanoparticles incorporated. The effect of the growth atmosphere composition on the quality of synthesis products is investigated. Indications provided by RS are confirmed by the results of scanning electron microscopy (SEM) and high-resolution transmission electron microscopy (HRTEM) analyses. Raman QI agreeably correlate with the average growth rate of the carbonaceous species.

1. Introduction

Raman spectroscopy, widely employed in the non-destructive analysis of the structural properties of all the C-based materials, may offer a valuable aid also in diagnostics of carbon nanotubes. CNT vibrational-properties have been deeply investigated and still represent a hot topic [1-11].

Far from getting deeper insight in this subject, this work demonstrates that the basic characteristics of CNT, such crystalline quality and phase purity, can be monitored by the use of quality indicators derived from Raman spectra decomposition. This is accomplished by morphologically and structurally analysing multi-walled nanotubes (MWCNT) prepared by Fe-catalysed CVD at 750 °C in C_2H_6+H_2 atmosphere. Raman QI displaying level of defectiveness and degree of smoothness of CNT, as well as, relative amount of catalyst inclusions are derived, and their reliability is tested by comparison with the results of the complementary SEM and HRTEM characterisation. By the aid of these parameters, the effect of the use of different hydrocarbon (HC) fractions on the CNT quality is investigated.

The picture emerging is that the increase of the HC-fraction in the growth atmosphere provokes the gradual loss of the CNT synthesis process selectivity. As a consequence, CNT result externally coated by an amorphous layer of increasing thickness. Conversely, the catalyst incorporation within the tubes progressively diminishes allowing the achievement of higher yields.

Table 1. Growth conditions: Φ_H, Φ_{HC} and x_{HC} denote respectively flow-rates of hydrogen and hydrocarbon and hydrocarbon fraction. Carbon yield (Y_C) and average C precipitation rate (ACPR) correspondingly attained are further reported, together with the average size of graphitic crystallites (L_C), as estimated from RS analysis results.

Sample	Φ_{HC}, cc/min	Φ_H, cc/min	x_{HC}	Y_C, wt.%	ACPR, μg/s	L_C, nm
#201	30	90	0.25	20.7	33	4.6
#202	60	60	0.50	34.7	55	4.5
#203	90	30	0.75	67.7	108	3.7
#204	120	0	1.00	82.0	132	3.0

2. Experimental details

The silica support is crushed and sieved and a fraction of 80–150 mm is retained for catalyst preparation. The catalyst is synthesised using an aqueous solution of $Fe(NO_3)_3 \cdot 9H_2O$ (20 wt.% Fe). The oxidic form of the iron catalyst (IC) precursor is obtained by calcination in air at 450 °C for 2 h, after wet solid drying at 100 °C. The catalyst (1.00±0.01g) is then placed in a ceramic boat inside the horizontal quartz reactor (length 60 cm, ∅ 3 cm), located in an electrical furnace, and flushed for 30 min in flowing pure hydrogen at RT and finally reduced at 650°C for 10 min. The hydrogen flow is then replaced by a mixture of ethane (carbon source) and hydrogen (carrier gas). Flow rates of C_2H_6 and H_2 utilised are reported in Tab.1. The synthesis is carried out at 750 °C for 1.75 h. Carbon yield, $Y_C(\text{wt.}\%) = 100 \cdot (M/M_0 - 1)$, is calculated by weighing reaction products (M) and catalyst after reduction (M_0). After synthesis, the SiO_2 support is removed with a solution of KOH (1 M) at 105 °C. Material attained, washed with distilled water and treated with a solution of HCl (1 M) in order to remove the remaining Fe-particles, is finally washed with distilled water and dried at 200 °C.

Raman scattering from pure CNT is measured by using an Instruments S.A. Ramanor U-1000 double monochromator equipped with an Olympus BX40 microscope for micro-Raman sampling. A X100 objective focuses the laser spot to a diameter of ~1 μm. A Hamamatsu R943-02 electrically cooled photomultiplier operating in photon-counting mode is used as a detection system. A Coherent Innova 70 Ar^+ laser operating at 2.41 eV provides excitation. Due to the weak Raman signal, a lot of spectra are recorded for each sample by integrating over 30 s for each point. The features detected in the 100–3100 cm^{-1} spectral range are fitted to Lorentzian bands superimposed to a constant background.

The morphological characterisation of the carbon deposits is carried out by SEM analyses on a JEOL JSM 5600LV instrument operating at 20 kV and equipped with an EDX analyser. HRTEM analyses are performed on a 200 kV JEOL JEM 2010 analytical electron microscope (LaB6 electron gun) equipped with a Gatan 794 Multi-Scan CCD camera for digital imaging and an Oxford Instrument (mod. 6498) for EDX analyses. Samples for TEM analyses are prepared by ultrasonic treatment in isopropyl alcohol for 2 min; subsequently, a drop of the suspension is dried on the standard TEM sample grid covered with holey carbon film.

3. Results of SEM, HRTEM and RS analyses

Figure 1 shows the effects produced by the changes of the growth atmosphere composition on the morphology of the thick and hollow MWCNT attained under conditions of Tab.1:

1) Gradual selectivity loss of CNT synthesis process;
2) Appearance of an amorphous layer on the external walls of the tubes, and;
3) Progressive diminishing of catalyst inclusions.

As can be seen, at lower hydrocarbon fractions (x_{HC}) CNT synthesis is highly selective (Fig.1a). CNT consist of quite smooth graphene layers (Fig.1b). Conversely, remarkable catalyst incorporation occurs (Fig.1c). With increasing x_{HC}, the average C precipitation rate (ACPR) increases (Tab.1) and amorphous phases start being co-produced (Fig.1d). An amorphous carbon (AC) layer of increasing

thickness coats tubular structures (Fig.1e). On the other hand, iron encapsulation, responsible for catalyst deactivation [12,13], reduces (Fig.1f), allowing the achievement of higher yields (Tab.1).

Typical Raman spectra of the samples under study are shown in Fig.2a. Three main groups of spectral features are detected within the probed range:

a) First-order (FO) bands arising from Csp^2 vibration modes (1200–1700 cm^{-1});
b) Corresponding second-order (SO) structures (above 2400 cm^{-1}), and;
c) Features originated from oxidic forms [14,15] of the IC encapsulated within the tubes (below 500 cm^{-1}).

All the samples exhibit similar FO and SO spectra. Instead, marked differences concern the IC-mode region (Fig.2b). The following Raman QI are derived from spectra decomposition:

1) D/G band intensity ratio (I_D/I_G), monitoring the structural disorder originating from the formation of defects in graphene layers and/or from AC inclusions [16-19];
2) Second-order/G-band intensity ratio (I_{SO}/I_G), displaying the average degree of crystalline perfection of C deposits (CD) [20];
3) Ratio between the intensities of the IC-features measured in sample and in bare catalyst (I_{CD}/I_{IC}), giving a measure of the extent of iron-nanoparticle encapsulation [15].

In Fig.2c, Raman QI are plotted as function of the average C precipitation rate. A good correlation is found. In particular, with increasing ACPR, I_D/I_G raises, while I_{SO}/I_G and I_{CD}/I_{IC} both diminishing, signalling that iron incorporation reduces, average defectiveness-level of graphene layers increases and their smoothness-degree diminishes.

4. Discussion

The results of quantitative analysis of Raman spectra demonstrate the crucial role played by the composition of the growth atmosphere in determining crystalline quality and phase purity of the C deposits. Trends shown in Fig.2c witness that the yield enhancement, produced by the diminished iron encapsulation attained upon gas-mixture HC-enrichment, is accompanied by a quality deterioration of the species synthesised. As exposed below, these findings are in agreement with the current assessments on the CNT growth.

The picture drawn by Raman QI is fully supported by the results of the morphologic analyses by SEM and HRTEM. No external amorphous layer is observed in sample #201 ($x_{HC} = 0.25$), while an AC layer coats external tube-walls of other samples. Its thickness increases from 2.5–3 nm in sample #202 ($x_{HC} = 0.50$), up to 7 nm in sample #204 ($x_{HC} = 1.00$). The increasing co-production of amorphous phases occurring towards higher x_{HC} gives rise to higher extent of structural disorder and lower crystalline perfection of graphene layers, as respectively displayed by the changes of I_D/I_G and I_{SO}/I_G ratios, and reflects onto the smaller average size of graphitic crystallites (Tab.1), as estimated from D/G intensity ratio via the Tuinstra-Koenig relationship [21].

This behaviour is agreeably understood as the effect of the higher growth rate achieved with gas-mixture HC-enrichment. In fact, it has been shown [22] that crystalline quality and phase purity of CNT prepared by catalytic process depend on the precipitation rates of CNT and of co-produced AC. At given reaction temperature and pressure, the deposition rates of the two allotropic phases increase with increasing the HC content of the growth-atmosphere. However, AC precipitation rate increases faster, thus explaining the observed selectivity loss of CNT growth process and the consequent quality worsening of C deposits.

The fragmentary dispersion of iron nanoparticles, induced by the large volume decrease of the solids accompanying the reduction process [23], has been recently proposed as the mechanism chiefly responsible for the iron-catalyst deactivation resulting in low CNT yields [12,13]. Indications coming out from I_{CD}/I_{IC} trend, confirmed by HRTEM observations, reveal a significant diminishing of IC incorporation in correspondence of the remarkable yield enhancement. Nevertheless, thermo-gravimetric measurements are currently in progress in order to quantitatively determine the amount of iron-particles encapsulated in CNT under the different growth conditions.

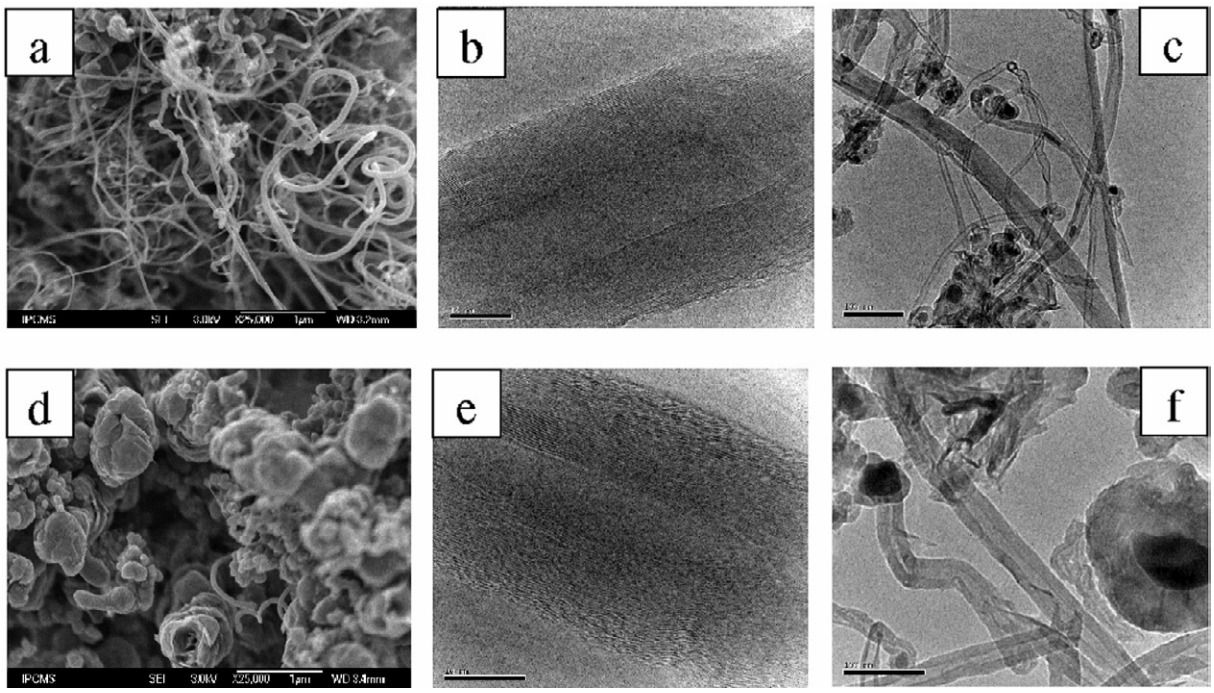

Figure 1. Morphology evolution evidenced by SEM (a,d) and HRTEM (b,c,e,f) analyses. Photos are taken after sample purification. Upper and lower images refer respectively to samples #201 and #204, grown using 0.25 and 1.00 hydrocarbon fractions x_{HC}. With increasing x_{HC}, the thickness of amorphous layer externally coating the tube walls increases, while the catalyst inclusions reduce.

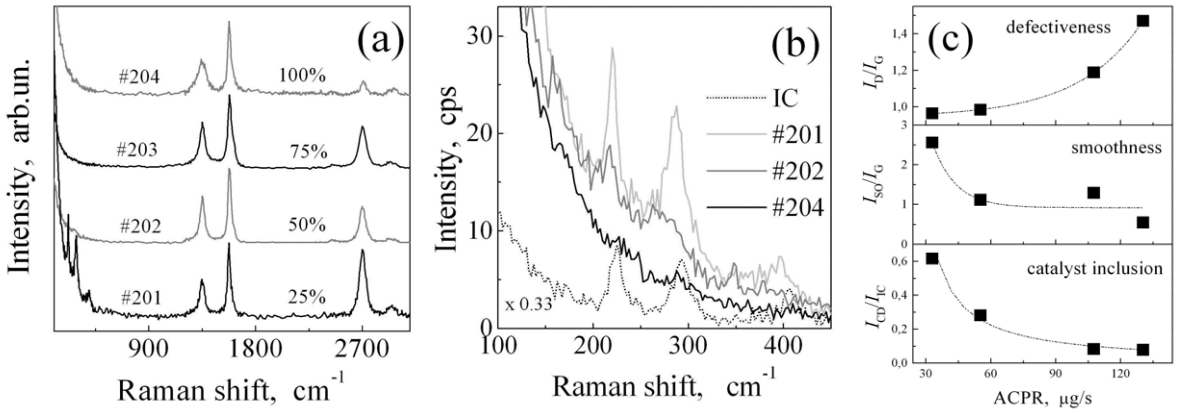

Figure 2. Results of Raman analysis. (a) Typical spectra of the investigated samples. The shape evolution, caused by the changes in ethane fraction (indicated), is evidenced by spectra normalisation to the maximum G-band intensity. Besides to the Csp^2 related first- and second-order structures, the features arising from iron catalyst (IC) are detected in the low frequency region. (b) IC features as measured in samples and in bare catalyst. (c) Raman quality-indicators as a function of average C precipitation rate (ACPR): defectiveness-level and smoothness-degree of C deposits (CD), and relative amount of catalyst inclusions, as respectively described by the D/G band (I_D/I_G), second-order/G-band (I_{SO}/I_G) and low-frequency features sample/catalyst (I_{CD}/I_{IC}) integrated intensity ratios. Lines are drawn to guide the eye.

5. Conclusion

This work

i) proposes the derivation of three quality indicators (QI) by the quantitative analysis of the Raman spectra of C nanotubes;
ii) tests their reliability by comparatively discussing the results obtained by complementary characterisation techniques (namely, SEM and HRTEM analyses); and
iii) suggests their use as a practical aid for quick post-growth diagnostics, particularly helpful in case of CNT synthesised by iron-catalysed process.

MWCNT prepared at 750°C by CVD in C_2H_6+H_2 atmosphere over 20%Fe/SiO_2 catalyst are considered as an example, and by decomposing their 2.41 eV spectra the following QI are derived: 1) D/G band intensity ratio, 2) second-order/G-band intensity, and 3) ratio between the intensities of the features arising from iron catalyst, measured in sample and in bare catalyst.

The latter Raman QI gives a measure of the extent of Fe-nanoparticle encapsulation and its use concerns exclusively the diagnostics of CNT grown by iron-catalysed process. Instead, the former two parameters, able to monitor average defectives-level and smoothness-degree of graphene layers, can be extensively used with all CNT, independently of the method utilised for their preparation.

By the aid of these QI, the crucial role, played by the composition of the growth atmosphere in determining crystalline quality and phase purity of the C deposits, is here demonstrated. The yield enhancement, produced by the (diminished Fe-encapsulation and consequently) reduced catalyst-deactivation attained upon gas-mixture hydrocarbon-enrichment, is accompanied by a quality deterioration of the species produced, which is understood as the effect of the higher growth rate, involving the increase of carbon precipitation in amorphous phase.

References

[1] A.M.Rao, S.Bandow, E.Ritcher, P.C.Eklund, Thin Solid Films 331 (1998) 141-147
[2] J.Kürti,H.Kuzmany, B.Burger, M.Hulan J.Winter G.Kresse, Synth. Met. 103 (1999) 2508-2509
[3] M.S.Dresselhaus, G.Dresselhaus, A.Jorio et al., Carbon. 40 (2002) 2043-2061
[4] R.Pfeiffer, H.Kuzmany, W.Pank, T.Pichler et al., Diam. Relat. Mater. 11 (2002) 957-960
[5] X.Zhao, Y.Ando, L.-C.Qin, H.Kataura,Y.Maniwa, R.Saito, Chem. Phys. Lett. 361 (2002) 169-174
[6] J.M.Benoit, J.P.Buisson, O.Chauvet, C.Godon, S.Lefrant, Phys. Rev. B66 (2002) 73417-4
[7] Z.Wang, X.Huang, R.Xue, L.Chen, J. Appl. Phys. 84 (1998) 227-231
[8] V.W.Brar, Ge.G.Samsonidze, M.S.Dresselhaus et al., Phys. Rev. B66 (2002) 155418-10
[9] M.S.Dresselhaus, G.Dresselhaus, R.Saito, A.Jorio, Phys. Reports 409 (2005) 47-99
[10] T.Shimada, T.Sugai, C.Fantini, M.Souza, L.G.Cançado et al., Carbon 43 (2005) 1049-1054
[11] C.Castiglioni et al., in "Carbon: the future material for advanced technology applications", G.Messina, S.Santangelo Eds., Springer's series Topics in Applied Physics 100, Heidelberg (2006) pp. 403-426
[12] M.A.Ermakova, D.Y.Ermakov, A.L.Chuvilin, G.G.Kuvshinov, J. Catal. 201 (2001) 183-197
[13] B.Louis, G.Gulino, R.Vieira, J.Amadou, T.Dintzer et al., Catalysis Today 102-103 (2005) 23-28
[14] www.chem.ucl.ac.uk/resources/raman/speclib.htlm
[15] M.G.Donato, G.Messina, S.Santangelo, M.Lanza, C.Milone, A.Pistone, in preparation
[16] G.Maurin, I.Stepanek, P.Bernier , J.-F.Colomer, J.B.Nagy et al., Carbon 39 (2001) 1273-1278
[17] R.Saito, A.Jorio, A.G.Souza Filho, A.Grüneis, M.A.Pimenta et al., Phys. B323 (2002) 100-106
[18] S.Cui, R.Canet, A.Derre, M.Couzi, P.Delhaes, Carbon 41 (2003) 709-809
[19] Md.Shajahan,Y.H.Mo, A.K.M.Fazle Kibria, M.J.Kim, K.S.Nahm, Carbon 42 (2004) 2245-2253
[20] Y.A.Kim, T.Hayashi,K.Osawa, M.S.Dresselhaus, M.Endo, Chem. Phys. Lett. 380 (2003) 319-324
[21] F.Tuinstra, J.L.Koenig, J. Comp. Mater. 4 (1970) 492-9
[22] M.Grujinic, G.Cao, B.Gertsen, Appl. Surf. Sci. 191 (2002) 223-239
[23] C.Emmenegger, J.-M.Bonard, P.Mauron, P.Sudan et al., Carbon 41 (2003) 539-547